Detecting and forecasting complex nonlinear dynamics in spatially structured catch-per-unit-effort time series for North Pacific albacore (*Thunnus alalunga*)

Sarah M. Glaser, Hao Ye, Mark Maunder, Alec MacCall, Michael Fogarty, and George Sugihara

Abstract: The presence of complex, nonlinear dynamics in fish populations, and uncertainty in the structure (functional form) of those dynamics, pose challenges to the accuracy of forecasts produced by traditional stock assessment models. We describe two nonlinear forecasting models that test for the hallmarks of complex behavior, avoid problems of structural uncertainty, and produce good forecasts of catch-per-unit-effort (CPUE) time series in both standardized and nominal (unprocessed) form. We analyze a spatially extensive, 40-year-long data set of annual CPUE time series of North Pacific albacore (*Thunnus alalunga*) from $1^\circ \times 1^\circ$ cells from the eastern North Pacific Ocean. The use of spatially structured data in compositing techniques improves out-of-sample forecasts of CPUE and overcomes difficulties commonly encountered when using short, incomplete time series. These CPUE series display low-dimensional, nonlinear structure and significant predictability. Such characteristics have important implications for industry efficiency in terms of future planning and can inform formal stock assessments used for the management of fisheries.

Résumé : La présence d'une dynamique complexe et non linéaire dans les populations de poissons et l'incertitude concernant la structure (forme fonctionnelle) de cette dynamique posent des défis en ce qui à trait à l'exactitude des prédictions faites par les modèles traditionnels d'évaluation des stocks. Nous décrivons deux modèles non linéaires de prédiction qui recherchent les signes d'un comportement complexe, évitent les problèmes de l'incertitude structurale et produisent de bonnes prédictions de séries chronologiques de captures par unité d'effort (CPUE) à la fois de forme standardisée et de forme nominale (non traitée). Nous analysons une banque de données à large représentation spatiale couvrant 40 années de séries chronologiques annuelles de CPUE de germons (*Thunnus alalunga*) du Pacifique Nord provenant de cellules de $1^\circ \times 1^\circ$ de l'est du Pacifique Nord. L'utilisation de données à structure spatiale dans les techniques de composition améliore les prédictions de CPUE au-delà des échantillons et surmonte les difficultés couramment rencontrées à l'utilisation de séries chronologiques courtes et incomplètes. Ces séries de CPUE possèdent une structure à faible dimension et non linéaire et une prédictibilité significative. De telles caractéristiques sont de grande importance pour la planification efficace future par l'industrie et peuvent enrichir les évaluations formelles de stocks utilisées dans la gestion des pêches.

[Traduit par la Rédaction]

Introduction

Marine populations typically vary across a broad spectrum of space and time scales. Understanding the causes of population fluctuations and their implications for management remains a primary objective of fisheries research (Sissenwine 1984; Sissenwine et al. 1988). Observed patterns of variability in marine populations have been classified along a continuum from steady state to "irregular" and "spasmodic" dynamics (Caddy and Gulland 1983; Spencer and Collie 1997). It has long been recognized that both nonlinear population processes and environmental forcing can generate dra-

Received 23 December 2009. Accepted 1 November 2010. Published on the NRC Research Press Web site at cjfas.nrc.ca on 10 February 2011.
J21583

Paper handled by Associate Editor Ray Hilborn.

S.M. Glaser,[1,2] H. Ye, and G. Sugihara. Scripps Institution of Oceanography, University of California, San Diego, La Jolla, CA 92093-0202, USA.
M. Maunder. Inter-American Tropical Tuna Commission, La Jolla, CA 92037-1508, USA.
A. MacCall. National Oceanic and Atmospheric Administration, National Marine Fisheries Service, Southwest Fisheries Science Center, Fisheries Ecology Division, Santa Cruz, CA 95060, USA.
M. Fogarty. National Oceanic and Atmospheric Administration, National Marine Fisheries Service, Northeast Fisheries Science Center, Woods Hole, MA 02543, USA.

[1]Corresponding author (e-mail: sglaser@ucsd.edu).
[2]Present address: Department of Ecology and Evolutionary Biology, University of Kansas, Lawrence, KS 66047, USA.

matic fluctuations in recruitment of marine fish and invertebrate stocks. Ricker (1954) provided the first demonstration of the potential for what is now called chaotic population dynamics in highly nonlinear systems, memorably describing the transition to chaos as involving "increasingly violent oscillations" in recruitment.

Nonlinear population dynamics can result from a variety of sources, including (*i*) multiplicative interactions between species or with physical variables (Dixon et al. 1999); (*ii*) high intrinsic growth rates with regulatory time lags (May 1976; Anderson et al. 2008); (*iii*) stochastic process noise or nonlinear amplification of stochastic physical forcing (Dixon et al. 1999; Sugihara 1994); (*iv*) low-frequency environmental variability driving a system across multiple stable states (Steele and Henderson 1984); (*v*) the tendency for large pelagic fishes to track low-frequency variability while "smoothing" high-frequency variability (Steele and Henderson 1984); or (*vi*) density-dependent dynamics, such as mortality and growth at early life history stages, interacting on multiple time and space scales (Royer and Fromentin 2006). Bakun (2001) outlined several fisheries-related observations consistent with the presence of nonlinear dynamics, such as the ephemeral nature of correlations with environmental variables and the failure of some collapsed populations to regain prior levels of productivity after fishery closures.

Nonlinear ecological interactions among components of the system and external perturbations due to natural and anthropogenic forcing factors have the potential to result collectively in extremely complex dynamics. Human interventions related to fishing intensity in response to economic forces (Berryman 1991; Conklin and Kolberg 1994), management strategies directed at size- and species-selective harvesting (Basson and Fogarty 1997), and remedial action such as artificial enhancement (Fagen and Smoker 1989) all have been shown to affect the probability of observing complex dynamics, including chaos, in these systems. The hallmark of a complex adaptive system is variability and surprise (Scheffer et al. 2009) — the potential for multiple stable states and rapid transitions in system dynamics requires that adaptive management structures be put in place to cope with unanticipated change.

The recognition that time series of population estimates potentially contain the signature of complex dynamical behaviors that can be separated from measurement error and stochastic forcing has revolutionized our ability to dissect the underlying causes of fluctuations in populations (Sugihara and May 1990; Tsonis and Elsner 1992; Sugihara 1994). These methods have now been applied to a number of marine systems (Dixon et al. 1999; Hsieh et al. 2005; Anderson et al. 2008). The nonlinear time series analysis underlying this approach employs a flexible nonparametric model structure and does not depend on an a priori specification of the governing equations for the system. This holds great advantage in marine fishery systems where model or structural uncertainty is often difficult to identify and quantify (Fogarty et al. 1997). Structural uncertainty in critical population and ecological processes (and in how they may change over time) can substantially degrade our ability to develop forecasts of population and ecosystem states (Charles 1998; Breiman 2001).

Relevant indicators of change in complex fisheries systems include commonly observed metrics such as catch per unit effort (CPUE), used both directly as an index of abundance or indirectly as an auxiliary variable in population models (Maunder and Punt 2004). In this paper, we investigate the dynamics of juvenile North Pacific albacore (*Thunnus alalunga*) using CPUE time series from the eastern North Pacific Ocean commercial troll fishery. We explore the use of spatially disaggregated data to increase information density based on the time series composite method of Sugihara (Sugihara 1994; Sugihara et al. 1996; Hsieh et al. 2008). Our objective is to test for hallmarks of nonlinear dynamics in these series and to produce annual forecasts of CPUE at two scales: (*i*) the entire region covered by the data and (*ii*) individual spatial cells (described below). This general approach can serve as an important complement to other fishery modeling and assessment methods.

Materials and methods

Data

North Pacific albacore are a single stock of highly migratory tuna confined to the North Pacific basin. The juvenile and adult subpopulations tend to occupy distinct regions of the Pacific and are harvested by separate fisheries (Otsu and Uchida 1963; Childers and Betcher 2008). Spawning occurs in the central western North Pacific Ocean (Laurs and Lynn 1977), and juveniles migrate into the productive California Current System (CCS) or the Kuroshio Current System (Kimura et al. 1997). Juveniles reside in the CCS from late spring to late fall, where they are harvested by the US, Canadian, and Mexican surface fleets. This albacore population does not have a history of rapid depletions, but catch rates are highly variable on an annual scale (ISC (International Scientific Committee for Tuna and Tuna-Like Species in the North Pacific Ocean) 2007). Decadal-scale differences in population estimates generated hypotheses during the 2004 stock assessment (Stocker 2005) that the population may contain periods of low (1975–1989) and high (1990–2000) productivity; however, these trends were less pronounced in the following stock assessment (ISC 2007) and require further study.

We analyze catch (number of fish) and effort (boat-days) from the US commercial troll fishery for North Pacific albacore in monthly $1^\circ \times 1^\circ$ spatial coordinates (hereafter, cells) from 1966–2005. The fishery lands juvenile albacore (ages 1–4) and is geographically centered in the CCS, although effort can extend into the central North Pacific gyre (Fig. 1). Data were obtained from voluntary submissions of logbooks, with approximately 20% vessel coverage (ISC 2007). Annual CPUE (x_t) for each spatial cell (Walters 2003) was calculated by summing catch and effort from June to October, the primary fishing season when albacore are present in the CCS. Few cells contained complete time series. Of 1366 cells containing a possible 40 years of data, 138 cells contained at least 20 years of data, 39 cells contained at least 35 years, and only 7 cells contained all 40 years of data (Figs. 1 and 2). Analysis was performed on normalized (mean = 0, standard deviation (SD) = 1) first differences ($\Delta x = x_{t-1} - x_t$). Such transformation removes secular trends

Fig. 1. Spatial cells (1° × 1°) containing catch and effort data from the US commercial troll fishery for juvenile albacore, 1966–2005. Small markers, ≥1 year of data; large markers, ≥35 years of data.

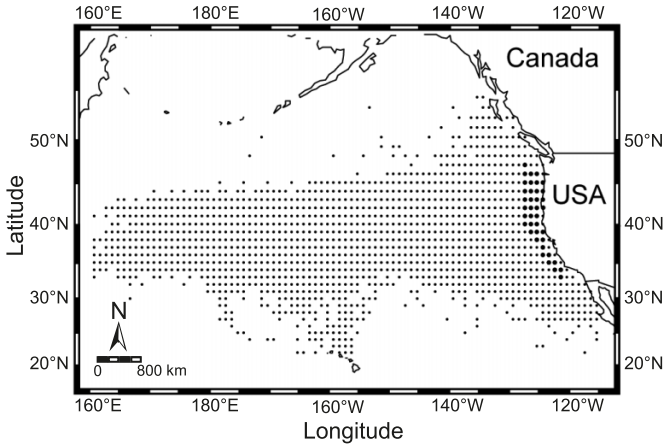

Fig. 2. Number of years with catch-per-unit-effort data in each of the 1366 spatial cells of juvenile North Pacific albacore harvested by the US commercial troll fishery, 1966–2005.

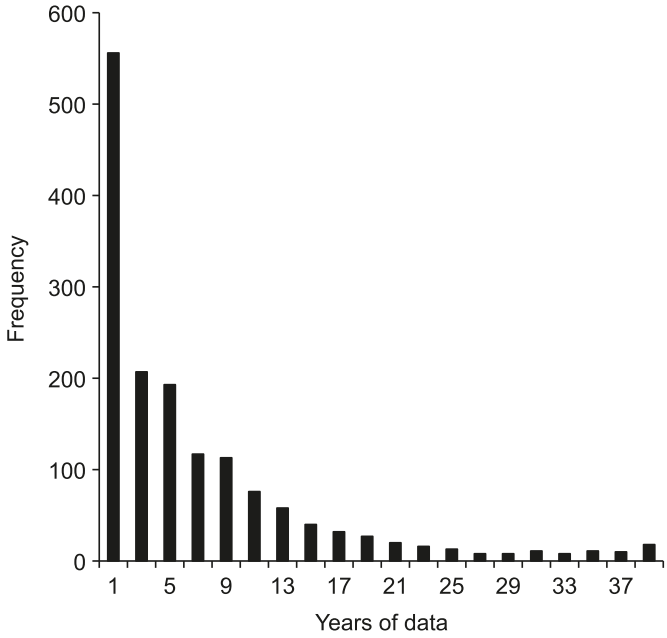

in data and allows compositing of series that may have different magnitudes and variances (described below).

Nonlinear forecasting

We define nonlinear dynamics as those for which the deterministic component $\phi(\boldsymbol{X})$ and the stochastic component $\phi(\varepsilon)$ are not additive, i.e., $\phi(\boldsymbol{X} + \varepsilon) \neq \phi(\boldsymbol{X}) + \phi(\varepsilon)$, and the resulting dynamics are unstable (exhibiting sensitive dependence on initial conditions). Nonlinear forecasting models are nonparametric statistical models that do not make assumptions about the underlying functional form of the system. Rather, they utilize the structure of the observed data itself to make forecasts. Consequently, one of their strengths is the ability to extract information about dynamical complex systems despite ignorance of the true dynamics. Another strength is that these models are parsimonious in their lack of free (fitted) parameters. For most applications, the basic model contains only one free parameter (dimensionality, as explained below).

Research has established these methods in a host of fields (Farmer and Sidorowich 1987; Casdagli 1992), including epidemiology (Sugihara and May 1990), cardiology (Sugihara et al. 1996), atmospheric science (Sugihara et al. 1999), ecology (Hsieh et al. 2005), behavior (Maye et al. 2007), and astronomy (Kilcik et al. 2009). However, they rarely have been used in fisheries science, despite the inherent complexity of and uncertainty about the systems under study. The two forecasting models described here, simplex projection and sequential locally weighted global linear maps (or S-maps), have complementary purposes; simplex projection calculates the dimensionality or degrees of freedom of the data (defined in the following paragraph), and S-maps classify the data as linear or nonlinear. Both models produce forecasts, and because they pose different questions about the data, the answers to which are ecologically important and relevant for modeling, we use them in concert.

The dynamics of a population are constrained by the action of N variables, or dimensions. In nature, these may be hundreds of physical and biological variables in the species' environment. A time series is merely a one-dimensional observation of the effects of those variables on the population. Fortunately, in dissipative (thermodynamically open) systems such as ecosystems, high-dimensional dynamics often collapse to simpler, low-dimensional dynamics, and a major part of the variability in the system can be modeled with relatively few variables (Schaffer and Kot 1985; O'Neill 1986; Crutchfield and McNamara 1987). The subset of these variables defines a state space in which each axis of the space corresponds to one variable, and in a dynamic system, the set of trajectories that define the movement of the observations in that space is called an attractor (Fig. 3). Over a sufficient time horizon, the path the observed variable traces within the state space defines the attractor, and perturbations to the system eventually return to that attractor. The geometry of these low-dimensional attractors can then be used to forecast the trajectory of an observed component variable, such as a targeted fish stock, by simply following the path of the attractor through time (Lorenz 1963).

We begin by identifying a small, thus tractable, set of dimensions for modeling that will result in the best predictability for the data. Typically, the key dimensions will be unknown variables; however, a mathematically similar version of the real attractor (a shadow attractor) can be constructed from time lags of the series, such that the lags represent the unknown variables. This is a direct implication of Takens' Theorem (Takens 1981), which demonstrates the lags of a time series can be used as proxies for the unknown dimensions shaping an attractor. These lags become axis coordinates, creating a univariate embedding that captures the characteristics of the real attractor (Takens 1981; Sugihara and May 1990). An embedding is simply the shadow attractor that results from plotting the time series against lags of itself, where each time-lagged axis is one dimension. A conceptual example of a time-lagged embedding is shown using observations of annual CPUE for juvenile North Pacific al-

Fig. 3. Time-lagged embedding for annual catch-per-unit-effort data from 43°N, 127°W, 1966–2005. (*a*) The time series shows changes in annual catch rate. (*b*) A two-dimensional plot of x_t versus x_{t-1} hints at underlying structure in the data. (*c*) A three-dimensional lagged-coordinate plot displays more coherent geometry, suggesting the presence of an attractor in the data.

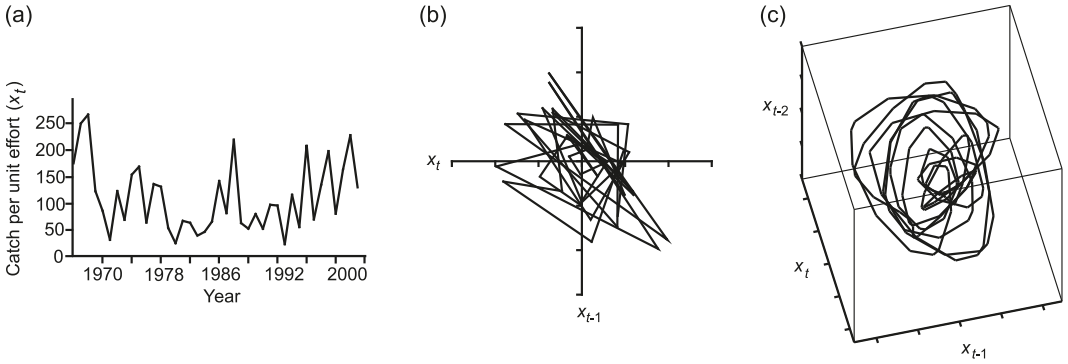

Fig. 4. Simplex projection (illustrated for $E = 2$, where E is the embedding dimension). We analyzed the data in increasingly higher dimensions (in this study, E ranged from 1 to 10), and the dimensionality that resulted in the highest forecast skill (ρ) or lowest mean absolute error (MAE) was chosen. (*a*) An embedding was created by plotting time lags of the data (for two dimensions, x_t versus x_{t-1}). The non-triangles are the set of library vectors from which the model was built. The triangle is the prediction vector that produced the forecast. The Euclidean distances between the prediction vector and all library vectors were calculated, and the E+1 nearest neighbors (black non-triangles) were selected. (*b*) The nearest neighbor library vectors (non-triangles) and prediction vector (triangles) are shown in relation to the one-dimensional time series. The one-step-ahead trajectory of the library vectors, x_{t+1} (non-triangles, connected by dashed line to library vector), determines the value of the forecast. (*c*) The forecast (*) is an exponentially weighted average of the E+1 nearest neighbor library trajectories, where trajectories are inversely weighted according to the distance of the nearest neighbor to the prediction in the embedding. Note the axes in panel (*c*) have been rescaled relative to panel (*b*) for clarity.

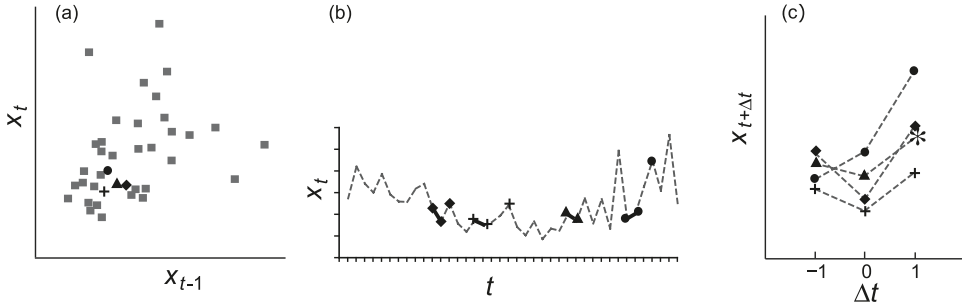

bacore (Fig. 3). The familiar one-dimensional time series (time, x_t) shows changes in annual catch rate. A two-dimensional embedding (x_{t-1}, x_t) begins to display a repeating pattern. In three dimensions (x_{t-2}, x_{t-1}, x_t), the geometry of the attractor becomes even more coherent.

In this study, nonlinear forecasting using CPUE time series was used to (*i*) calculate the number of dimensions needed to describe the time series; (*ii*) classify the time series as linear or nonlinear; and (*iii*) make 1-year-ahead forecasts. First, the simplex projection model (Sugihara and May 1990) identified the best embedding dimension (E) for the data. Second, this E-dimensional embedding was used in the S-maps model (Sugihara 1994) to assess the nonlinearity of the time series. Forecasts were produced using both models. The criteria for model performance is forecast skill (ρ, Pearson's correlation coefficient), measured as the correlation between observed and forecasted values, and mean absolute error (MAE), the absolute value of the difference between observed and predicted values. The nonlinear forecasting models are outlined briefly below. A more rigorous mathematical treatment of these methods can be found in Sugihara and May (1990) and Sugihara (1994).

Simplex projection

The simplex projection model is a nearest neighbor algorithm that uses the shape of the shadow attractor to follow the trajectory of the data when embedded in E-dimensions. We analyzed successively higher-dimensional embeddings (as in Fig. 3). For this study, we varied E from 1 to 10. The embedding creates vectors formed from the data of length E. One set of vectors is used to build the model, dubbed the library set, and a second set of vectors is used to test the ability of the model to make forecasts, dubbed the prediction set (see Fig. 4*a* for an example where $E = 2$). For any given prediction vector (Fig. 4*a*, triangle), the E+1 nearest neighbors are chosen from the library vectors (Fig. 4*a*, squares) based on the shortest Euclidean distances. The E+1 nearest neighbors are called the simplex (the minimum number of points required to surround a prediction vector in an E-dimensional space). The forward projection of the nearest neighbor vectors to time t+1 dictates the trajectory of the prediction vector to time t+1, generating the forecast (Fig. 4*c*, asterisk). The forecast is a weighted average of the nearest neighbor values at time t+1 with weights depending exponentially on the distance of the neighbors

Fig. 5. S-maps (illustrated for $E = 2$). As in simplex projection, an embedding is created by plotting time lags of the data (for two dimensions, x_t versus x_{t-1}). A global linear model is compared with locally weighted nonlinear models. The location of the prediction vector (triangle) is calculated based on the location of the library vectors (squares). In the linear model, equal weighting is applied to all library vectors in the embedding. In the nonlinear models, the library vectors are weighted exponentially according to their Euclidean distance from the prediction vector, with closer vectors receiving a higher weighting (background shading). The model becomes increasing more nonlinear according to the tuning parameter θ. The linear model is given by $\theta = 0$, and the nonlinear models are $\theta > 0$, so models are nested and equivalent.

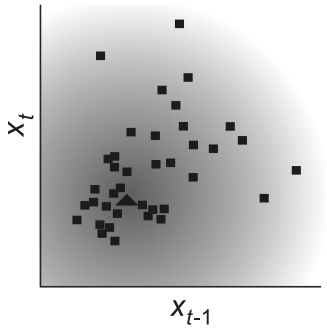

to the prediction vector at time t. That is, the weighting is determined at time t and applied to time t+1 for the forecast.

If the time series is long enough, the sets of library and prediction vectors are mutually exclusive (e.g., the first and second halves of the data). For short time series, we use cross-validation, for which only the prediction vector is held out of sample. The model accommodates missing values by excluding from the library or prediction sets any vector that would include a missing point. Forecasts for the prediction set are made at each time step, beginning with $x_{t+(E-1)}$ (to accommodate the length of the first vector). Forecast skill (ρ) and MAE are then calculated from the observed and forecasted values. As the geometry of the attractor changes with higher-dimensional embeddings (see Fig. 3), the library vectors defined as "nearest" may change. Thus, each successive embedding will produce different forecasts, and the E that results in the highest ρ and (or) lowest MAE is identified as the "best" embedding dimension for the data. In the majority of cases, the lowest MAE corresponds with the highest ρ. In cases in which there is a discrepancy, the metric that corresponds to the highest number of predictions (lowest E) is chosen. In our experience (unpublished data), cases in which there is a discrepancy in the best E identified by MAE and ρ occur for extremely noisy data, and the model ρ is rarely statistically significant (i.e., the model is not able to forecast the data). In simplex projection, E is the only free model parameter.

S-maps

S-maps classify a time series as linear or nonlinear based on the level of forecast skill obtained from equivalent linear or nonlinear models. The data are embedded based on the best E obtained using simplex projection. Again, the data are divided into sets of library vectors and prediction vectors (Fig. 5). The forecast is the location of the prediction vector at time t+1, calculated based on the locations of all the library vectors (in comparison with simplex projection, which uses only E+1 library vectors). In the global linear model, equal weighting is applied to all library vectors in the embedding. In the nonlinear models, the library vectors are weighted exponentially according to their Euclidean distance from the prediction vector, with closer vectors receiving a higher weighting when computing coefficients. A series of nonlinear models, with progressively greater weighting given to the localized neighborhood in the reconstructed state space, are analyzed.

S-maps produce forecasts governed by a nonlinear tuning parameter, θ. Specifically, for any given time step t, the set of library vectors is $\{\boldsymbol{x}_i\}$ (Fig. 5, squares) and the prediction vector is $\boldsymbol{x}_t$ (Fig. 5, triangle). The set of time series values at time $i + 1$ for library vectors is $\{y_i\}$, and the unknown forecast for $\boldsymbol{x}_t$ is $\hat{y}_t$. Setting $\boldsymbol{x}_t(0) \equiv 1$, then

$$\hat{y}_t = \sum_{j=0}^{E} \boldsymbol{c}_t(j)\boldsymbol{x}_t(j)$$

and $\boldsymbol{c}$ is solved by singular value decomposition (with a singularity threshold of 10^5) as

$$\boldsymbol{b} = \mathbf{A}\boldsymbol{c}$$

where $\boldsymbol{b}(i) = w(\|\boldsymbol{x}_i - \boldsymbol{x}_t\|)y_i$ and $\mathbf{A}(i, j) = w(\|\boldsymbol{x}_i - \boldsymbol{x}_t\|)\boldsymbol{x}_i(j)$ and

$$w(d) = \mathrm{e}^{-\theta d/\overline{d}}$$

where $w(d)$ is the weighting function, d is the Euclidean distance between a given library vector ($\boldsymbol{x}_i$) and the prediction vector ($\boldsymbol{x}_t$), and $\overline{d}$ is the mean Euclidean distance between all neighboring vectors (Sugihara 1994). For the matrix $\mathbf{A}$, j corresponds to the E time lags in each library vector such that each library and prediction vector has length E.

The model becomes increasingly nonlinear according to the tuning parameter θ. Note that the linear model is simply $\theta = 0$ and the nonlinear models are $\theta > 0$, so the models are nested and equivalent. For the linear model, an S-map is essentially an autoregressive model of order E, for which the same coefficients apply to each prediction vector. For $\theta > 0$, new coefficients are calculated for each prediction vector with weights depending on where the vector is in the reconstructed state space. As θ increases, the forecasts rely more strongly on the values in the local neighborhood (represented by the darker shading in Fig. 5). The data are nonlinear if greater weighting of the local neighborhood of library vectors results in a better model than that achieved from equally weighting all data (Casdagli 1992; Sugihara 1994). In S-maps, both E and θ are free parameters.

As with simplex projection, the best model produces the highest out-of-sample forecast skill (ρ) and (or) lowest error (MAE). The degree of nonlinearity is measured as $\Delta\rho_\theta = \rho_{\theta=\text{best}} - \rho_{\theta=0}$ and $\Delta\text{MAE}_\theta = |\text{MAE}_{\theta=\text{best}} - \text{MAE}_{\theta=0}|$. The significance of $\Delta\rho_\theta$ is measured with Fisher's Z test; with time series that contain significant serial autocorrelation (as with these CPUE data), $\Delta\rho_\theta$ can be a biased measure of nonlinearity (Hsieh and Ohman 2006). We therefore test the significance of the improvement in error, ΔMAE_θ, with a randomization procedure outlined in Hsieh and Ohman (2006). ΔMAE_θ for the model is calculated and treated as a

test statistic. Then, the order of the time series is shuffled, S-maps are used to model the shuffled time series, and a new ΔMAE_θ is calculated. This procedure is repeated 500 times to create a null distribution for ΔMAE_θ, against which the significance of the test statistic is measured. A series was classified as nonlinear if the significance of ΔMAE_θ exceeded $\alpha = 0.1$.

Formation of composite attractors

The dimensionality and forecast skill achieved with these methods is not absolute but is related to the amount and quality of the data available (i.e., the length of the time series and the amount of observational error). Short time series, often characteristic of CPUE data, may have low predictive skill and make identification of the dynamics (e.g., linear versus nonlinear, high-dimensional versus low-dimensional) difficult. This difficulty may be overcome by combining spatially structured CPUE series in a way that exploits the amount of data available. Specifically, time series from many spatial cells are combined into one composite library set, so that the embeddings are generated from all individual time series, resulting in a denser attractor. This has the net effect of increasing the length of time over which we have observed the dynamics, allowing us to see the system in more (and different) states than with a single time series.

We investigate the effect of using composite libraries to produce nonlinear forecasts for these CPUE data. Regarding these models, there is no rule defining the length of a time series required for sufficient information; forecast skill is a function of the levels of observation noise, the underlying complexity (E), and the degree of nonlinearity in the data. Forty years of data (available here) may produce good forecasts if the system is low-dimensional and the data contain a strong signal. However, if 40 years are insufficient, compositing can greatly enhance the underlying signal in the data without altering the dynamics contained in the individual series (Hsieh et al. 2008). By contrast, simple averaging or other linear transformations of data have been shown to obscure dynamics (Sugihara et al. 1990, 1999).

This compositing approach, used to analyze human heart rhythms (Sugihara et al. 1996), validated with model data, and applied to a multispecies ichthyoplankton data set (Hsieh et al. 2008), is appropriate if a key assumption is met: that all time series included in the composite are generated by the same dynamic process at some level of resolution (scale). It is likely the case of this albacore subpopulation (same fishery, region, and age group) that different time series are realizations of the same underlying processes that govern CPUE dynamics. Because albacore are highly migratory and the same subpopulation moves in and out of cells, time series from any given cell contains CPUE information that was likely to be generated by the same dynamics that govern the entire subpopulation. Even if albacore abundance or environmental conditions (e.g., temperature, forage) vary between cells, the underlying dynamic process may still be the same, in which case the time series need only to be scaled (normalized). We pose a specific test for this hypothesis: if the forecast skill of the model is improved when a composite library is used, then the dynamic process is homogeneous. If the dynamics are different, the inclusion of time series from heterogeneous processes would not improve forecast skill (and, in fact, might decrease it).

One goal of this study is to produce forecasts of CPUE at two spatial scales: the entire region and individual cells. The former was accomplished by creating a composite from all 1366 time series, providing a baseline for how well the model can simultaneously forecast the full data set. The latter was accomplished by comparing two approaches: (*i*) using the data from a single cell to forecast itself (where $n \leq 40$ years and using cross-validation) or (*ii*) using a composite library built from other cells to forecast (out-of-sample) the time series in a single target cell. The first approach is limited by the amount of data in any given cell, whereas the second approach will not produce good forecasts if other cells confound the signal (i.e., dynamics are heterogeneous).

We therefore examined three configurations of the time series. First, a composite built from all 1366 cells that contained data was analyzed as a whole; this is referred to as the full-composite. The full-composite describes the dynamics of the subpopulation at the scale of the sampling region and provides a baseline for comparing results from single cells (and for comparing analyses of the standardized time series, described below). Second, single cells were analyzed by forecasting themselves (dubbed single cell analysis). For each cell, E and θ were determined independently. Given the constraints imposed by short and incomplete time series, we selected the 39 cells that contained at least 35 years of data for this analysis. Third, a composite library set was constructed from 1365 cells, forecasting one excluded target cell; this is referred to as the target-composite. The target cells were the same 39 data-rich cells used in the single cell analysis. This third configuration tested whether a composite library improved the model forecast skill in comparison with a library generated from data in the single cell only.

In all analyses, forecasting was performed out-of-sample. In both the full- and target-composites, all occurrences (from other cells) of the year in the prediction vector were excluded from the library. That is, if the model was predicting the year 1977 in the target cell, all occurrences of 1977 were excluded from the composite library. The full-composite was long enough also to be divided into a library half and a prediction half (each containing 683 time series). Because results may vary depending on which series are in the library or prediction halves of the composite, we randomly shuffled the time series between library and prediction halves (500 times) and computed average statistics for the full-composite. In the case of the target-composites, the library (1365 cells) and prediction (1 cell) sets were mutually exclusive. Finally, when analyzing single cells, cross-validation was used so that the prediction vector was excluded from the library set.

Standardized CPUE

Estimates of albacore population size generally rely on fishery-dependent CPUE observations (Stocker 2005; ISC 2007), a measurement that can provide a relative index of abundance if certain assumptions are met. The primary assumption is that local catchability, or the fraction of fish in the environment caught by one unit of effort, remains constant as data are analyzed at different time and space scales.

This assumption is frequently violated (Harley et al. 2001), and methods for standardizing CPUE time series are designed to remove the confounding effects of variables exogenous to abundance that could systematically affect observations of CPUE (Maunder and Punt 2004). Standardization methods model CPUE as a function of independent variables; these typically include obvious influential factors such as time (e.g., year, month, season) and spatial location (e.g., latitude, longitude, distance from shore), but they can also include variables such as sea surface temperature, gear type, fishing nation, vessel information, etc. The statistical year effect produced from the model is the standardized CPUE, a single time series that represents assimilated data for an entire spatial domain. Thus, in addition to analysis of the nominal data described above (annual catch divided by annual effort in a cell), in this study we also consider a standardized CPUE series because they are frequently used in stock assessment models and as such may have immediate utility.

We implement a generalized linear model (GLM), the most common standardization method in use, to produce one standardized time series for the full data set. The model and data treatment were chosen based on the method used in albacore stock assessment (ISC 2007), described in McDaniel et al. (2006). Data were filtered to remove points with fewer than 3 days of total effort in a given cell-month. The model was $\log_e(\mathrm{CPUE}_{ijk} + 1) = \mathrm{year}_i + \mathrm{season}_j + \mathrm{area}_k + \varepsilon_{ijk}$, where "year" is 1966–2005; "season" is spring (April–May–June), summer (July–August–September), or fall (October–November–December); "area" is offshore (west of 130°W longitude) or inshore; and $\varepsilon \sim N(0, \sigma^2)$. The coefficients estimated for the year effect were back-transformed from logarithms for nonlinear forecasting.

The GLM was investigated in two ways, analogous to the approach used with (nominal) single cells. First, we analyzed the GLM as a single series (i.e., the series predicting itself using cross-validation; dubbed GLM-single) to investigate whether the dynamic complexity of the nominal CPUE data was preserved through the data assimilation that occurs with standardization. Second, the full-composite of 1366 nominal series was used as a library to predict the standardized CPUE (dubbed GLM-composite). This was done to see if the data-rich attractor reconstructed from the compositing of these extensive spatially resolved data could be used to improve forecasts of the standardized CPUE.

Results

The statistics for all configurations of the data are summarized (Table 1). Time series of nominal CPUE for juvenile North Pacific albacore exhibit low-dimensional, weakly nonlinear structure. The full-composite identified $E = 5$ (rounded from a mean of 4.7 over all 500 shufflings) as the best embedding dimension using simplex projection and classified the time series as nonlinear using S-maps. After excluding from the model vectors that would contain a missing data point, over 1000 forecasts were produced.

In general, use of the target-composite library to forecast individual cells produced better forecasts than the single cell analysis (Fig. 6). For the 39 target cells, the composite library outperformed (based on higher forecast skill, ρ) the use of the single cell to forecast itself in 35 of 39 cells using simplex projection and in 27 of 39 cells using S-maps. Using simplex projection, the target-composite identified, on average, an E of 5, whereas the single cells predicting themselves identified a mean E of 3. The composite library also increased the likelihood of detecting a nonlinear signal in the data. Ten of 39 time series (including all seven complete time series) were identified as nonlinear when a single cell was used to forecast itself. However, using the composite library, the model identified 17 of 39 as nonlinear.

The GLM-standardized series also contained a nonlinear signature, but only when the composite library was used. The forecast model with the highest skill was produced from simplex projection using the standardized series to predict itself (GLM-single; Table 1). That is, for simplex projection, the use of the full-composite library (made of 1366 nominal time series) did not improve forecast skill. The GLM-single analysis identified $E = 2$, whereas the GLM-composite identified $E = 5$. We demonstrate how 1-year-ahead forecasts are produced with this method (Fig. 7). Because forecast skill was highest with simplex projection ($\rho = 0.8$), this model was used to generate a forecast for 2006 using the standardized time series from 1966 to 2005. Interestingly, the root mean squared error of the GLM model (McDaniel et al. 2006) was significantly higher than the root mean squared error associated with forecasting the GLM using simplex projection (0.61).

Discussion

The ability to model albacore in few dimensions suggests the dynamics of CPUE are primarily driven by a small number of key variables. Furthermore, these dynamics are (weakly) nonlinear and predictable, allowing future catch rates to be modeled. From Takens' Theorem (Takens 1981), the E needed to reconstruct the state space can be bounded by $D < E < 2D + 1$, where D is the dimensionality of the (true, unobserved) system attractor. An E of 5 (calculated for the full composite) therefore translates to system dimensionality of between 2 and 4 (Casdagli 1992; Sugihara 1994). Consequently, it should be possible to identify which oceanographic or biological variables influence catch rate (Dixon et al. 1999). Factors that may determine albacore local abundance or catchability (but have not been shown to regulate population abundance) include sea surface temperature, chlorophyll *a* concentration, and forage availability (Laurs and Lynn 1977; Polovina et al. 2001; Zainuddin et al. 2006).

The nonlinear signal detected in these data is weak but present at certain scales and if sufficient data are available. We find conclusive evidence of nonlinearity (statistically significant decreases in MAE) in the full-composite, 44% of the target-composites, 25% of the single cells, and in the GLM-composite. The ability to detect any nonlinearity at all is remarkable given the constraints of spatial scale (Sugihara et al. 1999), time series length (Hsieh et al. 2008), and the presence of observation noise (Sugihara 1994). For the seven complete time series available (40 years long), all were nonlinear. The degree of nonlinearity ($\Delta\rho$) was related to the length of the target time series being forecast (R^2 =

Table 1. Summary statistics for nonlinear forecasting models predicting albacore catch per unit effort (CPUE).

		Simplex projection				S-maps				
Data configuration	No. of forecasts	E	ρ	ρ p value	MAE	ρ	ρ p value	MAE	|ΔMAE|	ΔMAE p value
Full-composite	1009±147[a]	4.7±0.61[a]	0.46±0.01[a]	<0.0001[a]	0.64±0.01[a]	0.56±0.01[a]	<0.0001[a]	0.58±0.01[a]	0.02±0.003[a]	<0.01[a]
Target-composite	27±5.5[b]	4.9±2.4[b]	0.58±0.1[b]	39 of 39*	0.56±0.10	0.59±0.1[b]	39 of 39*	0.59±0.07[b]	0.04±0.04[b]	17 of 39**
Single cells	27±5.5[b]	2.8±2.0[b]	0.35±0.2[b]	24 of 39*	0.61±0.12	0.52±0.2[b]	36 of 39*	0.63±0.10[b]	0.02±0.03[b]	10 of 39**
GLM-single	38	2	0.80	<0.0001	0.50	0.63	<0.0001	0.62	0.0007	NS
GLM-composite	34	5	0.64	<0.0001	0.58	0.68	<0.0001	0.56	0.06	0.04

Note: E is embedding dimension; ρ is model forecast skill; mean absolute error (MAE) is model error; ΔMAE measures the improvement of the nonlinear over the linear model; GLM is generalized linear model. *, number of series with forecast skill significant at $\alpha = 0.05$; **, number of series with significant nonlinearity at $\alpha = 0.10$.

[a]Mean ± standard deviation (SD) of 500 randomizations.

[b]Mean ± SD of 39 series.

0.19, $p < 0.006$), suggesting we are missing the nonlinear signal in shorter time series.

Most time series describing biological populations contain a linear component convolved with a nonlinear component, and which component dominates depends critically on scale. For example, while individual cities in the UK exhibit highly nonlinear measles dynamics, when data are grouped for the country as a whole, the nonlinear signal disappears (as incoherent noise) because contact rates are dominated by uniform school openings and closures (Sugihara et al. 1990). Indeed, although the effects of scale should make the detection of nonlinearity difficult, the fact that nonlinearity is commonly observed in natural time series speaks to the dominance of the nonlinear signal when the correct scale is identified. Finally, for comparison, the degree of nonlinearity detected in these time series is comparable to that calculated for model output of a chaotic (intrinsic rate of increase, $r > 3.69$) logistic map with added noise (Hsieh et al. 2008). Thus, detecting nonlinearity can be subtle.

There is no definitive way to ground-truth abundance estimated from fishery-dependent catch and effort data; thus, there is no way to prove that these results reflect the "true" population dynamics of juvenile albacore (though we have proven that coherent and predictable CPUE dynamics exist). Nonetheless, in this case we feel confident that the nominal CPUE full-composite reflects the biological dynamics of the juvenile subpopulation. This is because at small spatial scales (e.g., the $1^\circ \times 1^\circ$ cells used here), the fundamental premise underlying the use of CPUE as an index of abundance holds most true: that catchability is relatively constant (Hinton and Maunder 2004). In the case of these data, for which gear type, fishing nation, target species, and albacore age distribution are constant, the primary confounding variables are time (month, season) and space (latitude, longitude). By confining analysis of nominal data to disaggregated cells with constant space and season, we effectively standardize the data to these independent variables. Each observed time series in a given spatial cell therefore represents the change from year to year in the fish being caught in that cell, potentially describing changes in migration or habitat. However, when the data from individual cells are combined in the composite library, the model has information from the full region from which to build the best forecast. Because the data are not averaged or summed, analysis of the full region maintains the signal found at small spatial and annual time scales (through the construction of library and prediction vectors that are limited to consecutive points in a given cell) while describing the dynamics at the scale of the subpopulation.

As further support, the improvement in forecast skill and decrease in error found when comparing the target-composites to single series suggests the composite model is capturing dynamics that exist at a larger spatial scale than individual cells. The information contained in a library of 1365 cells, when combined, is better able to forecast the dynamics in a single cell than that cell is at forecasting itself. If the dynamic process was fundamentally different across cells in the region, the highest forecast skill should be achieved with the single cell analysis because historical data from that cell would produce the best forecasts. The qualitative similarity (low-dimensional, nonlinear)

Fig. 6. The use of composite libraries (target-composite analysis described in text) significantly improved the ability of the model to forecast a catch-per-unit-effort (CPUE) time series in a single cell compared with using the single cell to forecast itself. The target-composite also identified a higher embedding dimension (E) for the data. Marker is calculated mean, error bars are standard error. Improvement of target-composite over single series was calculated by two-tailed paired t test ($n = 39$; *, $p < 0.01$; **, $p < 0.001$). (a) Best E identified by simplex projection, (b) forecast skill (ρ) achieved by simplex projection, (c) ρ achieved by S-maps, (d) mean absolute error (MAE) of forecasts by S-maps.

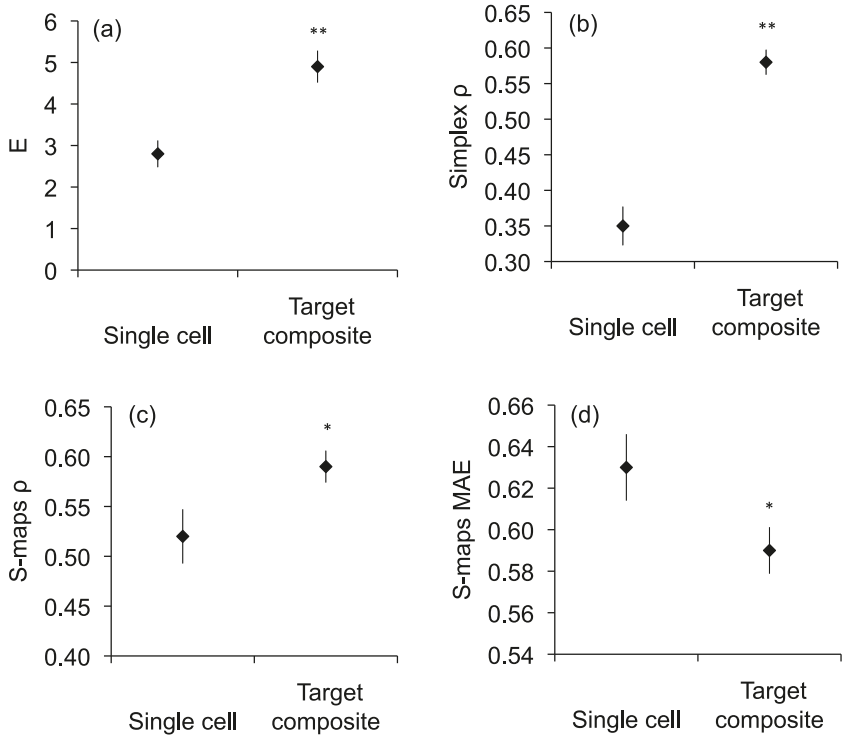

Fig. 7. The standardized catch-per-unit-effort (CPUE) time series from 1966 to 2005 was used to produce a forecast (*) for 2006. Simplex projection, the model producing the highest forecast skill, was used. Data were analyzed as normalized (mean = 0, standard deviation (SD) = 1) first differences. Solid line is observed data, dashed line is forecasted data.

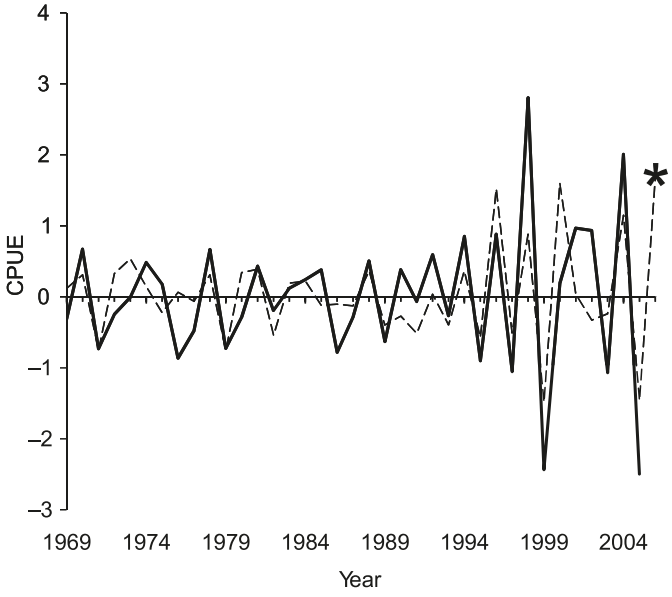

between the full-composite and mean values for the target-composites suggests the various configurations of scale converge on a coherent description of the data.

For nominal CPUE data, the application of composite methods overcomes challenges posed by short and incomplete time series. By combining many incomplete series, the model is more likely to find a sample of vectors long enough to test higher-dimension embeddings and the overall skill of the models is significantly higher. The composite approach also improves our ability to detect nonlinearity. Most (32 of 39) target time series contained at least one gap in the 40-year period. Of the seven complete time series, nonlinearity was detected in all of them. However, there was a 50% greater chance of detecting nonlinearity in the incomplete time series if a composite library was used. In summary, the repeated finding of nonlinearity in all complete single time series, nearly 50% of target-composites (with the accompanying higher forecast skill), in the full-composite and in the standardized data suggests the proper functional form is nonlinear.

For these data, the length of time series needed for skilful forecasts appears to be 33–35 years. Single cells containing 27 years of data were insufficient to identify nonlinearity, but those containing 33 years or more were identified as nonlinear. These findings are consistent with other studies comparing analysis of long and short time series using composite libraries, whereby forecasting of a known nonlinear model (even without observational noise) either did (n = 150 points) or did not (n = 30 points) detect that nonlinear-

Fig. 8. The logistic growth model ($\boldsymbol{x}(t) = r\boldsymbol{x}(t–1)[1 – \boldsymbol{x}(t–1)]$) becomes increasingly defined as each of five time series (40 points long) is added. Many points cluster, but the occurrences of rare points add critical information about the full shape of the function. Likewise, compositing dynamically similar, but mutually exclusive, time series leverages spatially defined catch-per-unit-effort data, using what might otherwise be considered redundant. For the model, $r = 3.5$, $\boldsymbol{x}_1(0) = 0.1$, $\boldsymbol{x}_2(0) = 0.007$, $\boldsymbol{x}_3(0) = 0.05$, $\boldsymbol{x}_4(0) = 0.2$, $\boldsymbol{x}_5(0) = 0.98$.

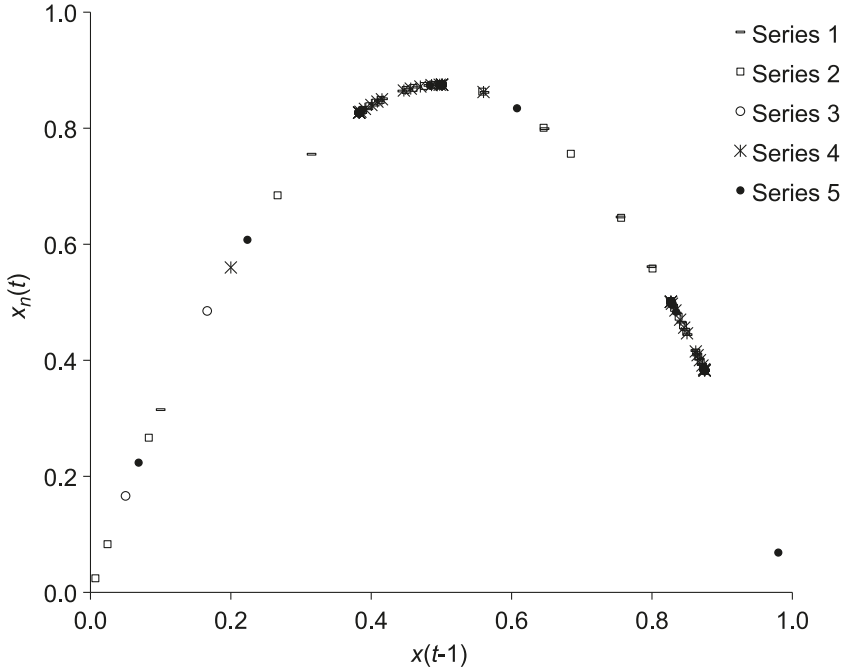

ity (Hsieh et al. 2008). Theoretically, the CPUE series with the most complete data (fewest gaps) correspond to areas of most regular fishing effort (and potentially highest fish abundance), making these cells likely to have lower observational noise than cells with incomplete series. Practically, the most complete time series also provide the model more information from which to build the attractor, as the neighborhood around the prediction vectors is denser.

Composite libraries add information to the reconstructed attractor that improves the model's ability to resolve forward trajectories or prediction vectors (Hsieh et al. 2008). In this study, the composite time series represent repeated samples or observations of the attractor describing the system in which albacore are harvested (samples of the process that are not identical). In the case of a multispecies composite (Hsieh et al. 2008), a time series provides a one-dimensional view of the attractor describing the community of interacting species. In the case of a single species composite, the individual time series can be thought of as iterations of the mechanistic model (e.g., a logistic population growth model) describing the fish population, but with different initial conditions (e.g., the (scaled) catch rate of fish in a cell at a given time). Each time series contributes information about the shape of the attractor; some of it is redundant, but some of it is new.

As a heuristic example, we demonstrate how the logistic population growth model (in canonical form), plotted as a two-dimensional embedding (also known as the logistic return map; May 1976), becomes more defined as successive, independent series with different initial conditions are plotted (Fig. 8). The parts of the function most densely filled with points represent values commonly observed (say, mean abundance levels, or in our case, mean catch rates). Such parts of the function are easily observed with only a few years of data from the first iteration. As points from less commonly observed parts of the function are added, critical (because they are rare) sections are filled in. In a similar fashion, the composite attractor created from 1366 time series spanning a large portion of the geographic distribution of juvenile albacore in the North Pacific includes information about the dynamics in areas of high catch rates (e.g., the time series in the CCS where albacore are densely aggregated and abundant), as well as in areas of low catch rates (e.g., in the migratory highway through the central gyre; Polovina et al. 2001). When combined, these time series produce a more defined attractor. Thus, this technique takes advantage of the large amounts of data available from spatially structured CPUE data sets to increase our ability to observe the full system attractor.

Analysis of the GLM-standardized time series presents two conclusions: data assimilation through standardization removes the nonlinear signal detected in the nominal data and reduces the complexity (dimensionality) of the dynamic process. Nonlinearity was detected only when the composite library of all cells (in nominal form) was used to forecast the standardized series. Furthermore, the GLM-single analysis found $E = 2$ as opposed to $E = 5$ with the composite (similar to the full-composite of nominal data). Given the goals of standardization, to reduce observation noise and remove the effects of confounding variables, this result is expected; the process of standardization effectively reduces the number of independent variables acting on the dependent variable, CPUE. For forecasting a standardized time series, the best model was simplex projection with an E of 2, using

the single series to forecast itself. The composite library did improve the forecast skill of S-maps, but the S-maps model produced less accurate forecasts than simplex projection.

This raises a critical point about the parameter *E*. As we use it here, *E* is not an absolute number that is intrinsic or invariant. Rather, the choice of *E* for a given model is operationally tied to the forecast skill that is practically achievable (given the amount of data and the observational noise). Embedding the time series in a given dimension produces a certain level of predictive skill that increases as the attractor is unwound, resolved so trajectories do not cross (i.e., singularities are resolved). Furthermore, while *E* can be thought of as corresponding to the axes in state space that affect the dependent variable (i.e., the critical driving variables in the system), there is not necessarily a one-to-one correspondence. In the case of our data, then, if the goal is to model the nominal time series, one would look for two to five variables to explain the system dynamics, with the aim of reproducing or surpassing the level of prediction skill attained with lagged coordinates. If the goal is to model the standardized time series, only two variables will be needed. The "missing" dimensions in the standardized series likely reflect the process of standardization itself. The difference between an *E* of 4 and an *E* of 5 is not the difference between a "correct" and an "incorrect" model. The important point is that the data sets can be modeled with relatively few dimensions.

This study provides a means of incorporating forecasts of time series containing nonlinear dynamics into stock assessment models and of supplementing current approaches to management. Most stock assessment models make forecasts, sometimes 10 years into the future, based on an equilibrium state estimated from historical data and with an additive stochastic component to replicate recruitment variability (for albacore, see Stocker 2005; ISC 2007). The population dynamics model is then evolved in time based on static coefficients, and the resulting biomass forecasts become asymptotic. Instead of basing the stock assessment forecast on stable dynamics, here we suggest that an annual CPUE forecast be used to drive the stock assessment model either by predicting catch rate for each individual cell or by predicting the trajectory of the standardized series. This would be particularly valuable for short-lived species (such as pollock (*Pollachius virens*) or Pacific cod (*Gadus macrocephalus*)) for which total allowable catch is updated every year based on annual assessments. Stock assessment models also produce short-term forecasts that could be directly compared with the output of our models. While the nonlinear methods do not make predictions many years into the future, for the purpose of management, 1-year-ahead forecasts are an important product. For species that are longer lived and where constant mortality assumptions are valid, these forecast methods can be used on annual recruits and extrapolated upward to create longer-term forecasts for the stock.

Equilibrium-based models of fisheries could fail to predict major population changes (Mangel et al. 2002). Nonlinear models, especially ones like these that are not constrained by distributional assumptions for variables such as mortality or spawner–recruit relationships, may provide more accurate (yet simpler) ways of modeling the dynamics of populations. Such flexibility in the model also overcomes structural uncertainty inherent in traditional population dynamics models. The choice between data models and algorithmic models does not have to be zero-sum (Breiman 2001); we advocate the use of both types of models to maximize biological understanding and forecast accuracy and to provide a means of validation. Finally, data compositing methods offer a technique complementary to standardization for analyzing CPUE data that is directly useful in management of marine fisheries. Both the composite analysis and the GLM are means of assimilating large amounts of data into a single estimate of stock size.

This approach is not a silver bullet for stock assessments. Most notably, in its current univariate form, forecasts are not provided as a function of varying levels of effort, a necessary feature when setting harvest guidelines (although effort changes can be accommodated with a multivariate approach; Dixon et al. 1999). Consequently, we see the information obtained from these methods as complementary to that obtained from stock assessment models that can produce proscriptive recommendations based on varying levels of catch or effort. Our approach makes distribution-free forecasts in a way that allows analysis of error in the model, but also captures the dynamic signature underlying the data and provides insight into the degree of complexity underlying the processes governing albacore dynamics.

In summary, the juvenile subpopulation of North Pacific albacore display low-dimensional, weakly nonlinear dynamics that can be forecast 1 year ahead. We add a new method to the suite of fisheries models that accounts for the nonlinear structure of natural populations and can be used to overcome limitations posed by short and incomplete CPUE time series. Further, we suggest that large data sets containing highly resolved, spatially structured CPUE data should not be treated as though individual time series contain only redundant information to be assimilated and averaged. Rather, such time series, even those on the geographic periphery of the species' range, contain valuable information about the dynamic structure of the population. The large data set available for North Pacific albacore demonstrates the usefulness of such a suite of data. Given the ability of low-dimensional nonlinear models to forecast changes in albacore CPUE, forecasts made at the level of CPUE time series should supplement those made by stable population dynamics models. Such an addition to current stock assessments will provide a baseline for active management of the population, indicators of (potentially important) future changes to population abundance, and a template for forecasting key subprocesses such as recruitment.

Acknowledgements

We thank L. Kaufman, E. Kline, E. Deyle, C. Hsieh, and C. Hendrix for valuable comments on drafts of this paper and A. Rosenberg, H. Liu, B. Fissel, M. Cape, S. Martin, B. Carr, C.H. Hsieh, and I. Altman for discussion of this approach. Funding was provided through NA08OAR4320894 and NA09NMF4720177, grants from the Comparative Analysis of Marine Ecosystem Organization (CAMEO) program, a partnership between the US National Science Foundation and NOAA National Marine Fisheries Service. This is contribution No. 5.

References

Anderson, C.N.K., Hsieh, C.H., Sandin, S.A., Hewitt, R., Hollowed, A., Beddington, J., May, R.M., and Sugihara, G. 2008. Why fishing magnifies fluctuations in fish abundance. Nature (London), **452**(7189): 835–839. doi:10.1038/nature06851. PMID:18421346.

Bakun, A. 2001. 'School-mix feedback': a different way to think about low frequency variability in large mobile fish populations. Prog. Oceanogr. **49**(1–4): 485–511. doi:10.1016/S0079-6611(01)00037-4.

Basson, M., and Fogarty, M.J. 1997. Harvesting in discrete-time predator–prey systems. Math. Biosci. **141**(1): 41–74. doi:10.1016/S0025-5564(96)00173-3. PMID:9077079.

Berryman, A.A. 1991. Can economic forces cause ecological chaos — the case of the Northern California Dungeness crab fishery. Oikos, **62**(1): 106–109. doi:10.2307/3545457.

Breiman, L. 2001. Statistical modeling: the two cultures. Stat. Sci. **16**(3): 199–231. doi:10.1214/ss/1009213726.

Caddy, J.F., and Gulland, J.A. 1983. Historical patterns of fish stocks. Mar. Policy, **7**(4): 267–278. doi:10.1016/0308-597X(83)90040-4.

Casdagli, M. 1992. Chaos and deterministic versus stochastic nonlinear modelling. J. R. Stat. Soc. B Met. **54**(2): 303–328.

Charles, A.T. 1998. Living with uncertainty in fisheries: analytical methods, management priorities and the Canadian groundfishery experience. Fish. Res. **37**(1–3): 37–50. doi:10.1016/S0165-7836(98)00125-8.

Childers, J., and Betcher, A. 2008. Summary of the 2007 U.S. North and South Pacific albacore troll fisheries. NOAA Admin. Rep. No. LJ-08-05.

Conklin, J.E., and Kolberg, W.C. 1994. Chaos for the halibut? Mar. Resour. Econ. **9**: 159–182.

Crutchfield, J.P., and McNamara, B.S. 1987. Equations of motion from a data series. Complex Systems, **1**: 417–452.

Dixon, P.A., Milicich, M.J., and Sugihara, G. 1999. Episodic fluctuations in larval supply. Science (Washington, D.C.), **283**(5407): 1528–1530. doi:10.1126/science.283.5407.1528. PMID:10066174.

Fagen, R., and Smoker, W.W. 1989. How large-capacity hatcheries can alter interannual variability of salmon production. Fish. Res. **8**(1): 1–11. doi:10.1016/0165-7836(89)90036-2.

Farmer, J.D., and Sidorowich, J.J. 1987. Predicting chaotic time series. Phys. Rev. Lett. **59**(8): 845–848. doi:10.1103/PhysRevLett.59.845. PMID:10035887.

Fogarty, M.J., Hilborn, R., and Gunderson, D. 1997. Chaos and parametric management. Mar. Policy, **21**(2): 187–194. doi:10.1016/S0308-597X(96)00050-4.

Harley, S.J., Myers, R.A., and Dunn, A. 2001. Is catch-per-unit-effort proportional to abundance? Can. J. Fish. Aquat. Sci. **58**(9): 1760–1772. doi:10.1139/cjfas-58-9-1760.

Hinton, M.G., and Maunder, M.N. 2004. Methods for standardizing CPUE and how to select among them. Col. Vol. Sci. Pap. ICCAT, **56**(1): 169–177.

Hsieh, C.H., and Ohman, M.D. 2006. Biological responses to environmental forcing: the linear tracking window hypothesis. Ecology, **87**(8): 1932–1938. doi:10.1890/0012-9658(2006)87[1932:BRTEFT]2.0.CO;2. PMID:16937630.

Hsieh, C.H., Glaser, S.M., Lucas, A.J., and Sugihara, G. 2005. Distinguishing random environmental fluctuations from ecological catastrophes for the North Pacific Ocean. Nature (London), **435**(7040): 336–340. doi:10.1038/nature03553. PMID:15902256.

Hsieh, C.H., Anderson, C.N.K., and Sugihara, G. 2008. Extending nonlinear analysis to short ecological time series. Am. Nat. **171**(1): 71–80. doi:10.1086/524202. PMID:18171152.

ISC. 2007. Report of the Albacore Working Group Workshop, 28 November – 5 December 2006, Shimizu, Japan. International Scientific Committee for Tuna and Tuna-Like Species in the North Pacific Ocean, National Research Institute of Far Seas Fisheries, Shizuoka-Shi, Japan. Available from http://isc.ac.affrc.go.jp/pdf/ISC7pdf/Annex_5_ALBWG_Nov2Dec_06.pdf.

Kilcik, A., Anderson, C.N.K., Rozelot, J.P., Ye, H., Sugihara, G., and Ozguc, A. 2009. Nonlinear prediction of solar cycle 24. Astrophys. J. **693**(2): 1173–1177. doi:10.1088/0004-637X/693/2/1173.

Kimura, S., Munenori, N., and Sugimoto, T. 1997. Migrations of albacore, *Thunnus alalunga*, in the North Pacific Ocean in relations to large oceanic phenomena. Fish. Oceanogr. **6**(2): 51–57. doi:10.1046/j.1365-2419.1997.00029.x.

Laurs, R.M., and Lynn, R.J. 1977. Seasonal migration of North Pacific albacore, *Thunnus alalunga*, into North American coastal waters — distribution, relative abundance, and association with transition zone waters. Fish. Bull. **75**(4): 795–822.

Lorenz, E.N. 1963. Deterministic nonperiodic flow. J. Atmos. Sci. **20**(2): 130–141. doi:10.1175/1520-0469(1963)020<0130:DNF>2.0.CO;2.

Mangel, M., Marinovic, B., Pomeroy, C., and Croll, D. 2002. Requiem for Ricker: unpacking MSY. Bull. Mar. Sci. **70**(2): 763–781.

Maunder, M.N., and Punt, A.E. 2004. Standardizing catch and effort data: a review of recent approaches. Fish. Res. **70**(2–3): 141–159. doi:10.1016/j.fishres.2004.08.002.

May, R.M. 1976. Simple mathematical models with very complicated dynamics. Nature (London), **261**(5560): 459–467. doi:10.1038/261459a0. PMID:934280.

Maye, A., Hsieh, C.H., Sugihara, G., and Brembs, B. 2007. Order in spontaneous behavior. PLoS ONE, **2**(5:e443): 1–14.

McDaniel, J.D., Crone, P.R., and Dorval, E. 2006. Critical evaluation of important time series associated with albacore fisheries (United States, Canada, and Mexico) of the eastern North Pacific Ocean. International Scientific Committee for Tuna and Tuna-Like Species in the North Pacific Ocean (ISC), National Research Institute of Far Seas Fisheries, Shizuoka-Shi, Japan. ISC/06/ALBWG/09.

O'Neill, R.V., Deangelis, D.L., Waide, J.B., and Allen, G.E. 1986. A hierarchical concept of ecosystems. Princeton University Press, Princeton, N.J.

Otsu, T., and Uchida, R.N. 1963. Model of the migration of albacore in the North Pacific Ocean. Fish. Bull. **63**(1): 33–44.

Polovina, J.J., Howell, E., Kobayashi, D.R., and Seki, M.P. 2001. The transition zone chlorophyll front, a dynamic global feature defining migration and forage habitat for marine resources. Prog. Oceanogr. **49**(1–4): 469–483. doi:10.1016/S0079-6611(01)00036-2.

Ricker, W.E. 1954. Stock and recruitment. J. Fish. Res. Board Can. **11**: 559–623.

Royer, F., and Fromentin, J.M. 2006. Recurrent and density-dependent patterns in long-term fluctuations of Atlantic bluefin tuna trap catches. Mar. Ecol. Prog. Ser. **319**: 237–249. doi:10.3354/meps319237.

Schaffer, W.M., and Kot, M. 1985. Do strange attractors govern ecological systems? Bioscience, **35**(6): 342–350. doi:10.2307/1309902.

Scheffer, M., Bascompte, J., Brock, W.A., Brovkin, V., Carpenter, S.R., Dakos, V., Held, H., van Nes, E.H., Rietkerk, M., and Sugihara, G. 2009. Early-warning signals for critical transitions. Nature (London), **461**(7260): 53–59. doi:10.1038/nature08227. PMID:19727193.

Sissenwine, M.P. 1984. Why do fish populations vary? *In* Exploitation of marine communities. *Edited by* R.M. May. Springer-Verlag, Berlin, Germany. pp. 59–94.

Sissenwine, M.P., Fogarty, M.J., and Overholtz, W.J. 1988. Some fishery management implications of recruitment variability. *In* Fish population dynamics. *Edited by* J.A. Gulland. J. Wiley and Sons, London, UK. pp. 129–152.

Spencer, P.D., and Collie, J.S. 1997. Effect of nonlinear predation rates on rebuilding the Georges Bank haddock (*Melanogrammus aeglefinus*) stock. Can. J. Fish. Aquat. Sci. **54**(12): 2920–2929. doi:10.1139/cjfas-54-12-2920.

Steele, J.H., and Henderson, E.W. 1984. Modeling long-term fluctuations in fish stocks. Science (Washington, D.C.), **224**(4652): 985–987. doi:10.1126/science.224.4652.985. PMID:17731996.

Stocker, M. (*Editor*). 2005. Report of the Nineteenth North Pacific Albacore Workshop, 25 November – 2 December 2004, Nanaimo, B.C., Canada. Fisheries and Oceans Canada, Pacific Biological Station, Nanaimo, B.C., Canada.

Sugihara, G. 1994. Nonlinear forecasting for the classification of natural time-series. Philos. Trans. R. Soc. A, **348**(1688): 477–495. doi:10.1098/rsta.1994.0106.

Sugihara, G., and May, R.M. 1990. Nonlinear forecasting as a way of distinguishing chaos from measurement error in time series. Nature (London), **344**(6268): 734–741. doi:10.1038/344734a0. PMID:2330029.

Sugihara, G., Grenfell, B., May, R.M., Chesson, P., Platt, H.M., and Williamson, M. 1990. Distinguishing error from chaos in ecological time-series. Philos. Trans. R. Soc. B, **330**(1257): 235–251. doi:10.1098/rstb.1990.0195.

Sugihara, G., Allan, W., Sobel, D., and Allan, K.D. 1996. Nonlinear control of heart rate variability in human infants. Proc. Natl. Acad. Sci. U.S.A. **93**(6): 2608–2613. doi:10.1073/pnas.93.6.2608. PMID:8637921.

Sugihara, G., Casdagli, M., Habjan, E., Hess, D., Dixon, P., and Holland, G. 1999. Residual delay maps unveil global patterns of atmospheric nonlinearity and produce improved local forecasts. Proc. Natl. Acad. Sci. U.S.A. **96**(25): 14210–14215. doi:10.1073/pnas.96.25.14210. PMID:10588685.

Takens, F. 1981. Detecting strange attractors in turbulence. Lect. Notes Math. **898**: 366–381. doi:10.1007/BFb0091924.

Tsonis, A.A., and Elsner, J.B. 1992. Nonlinear prediction as a way of distinguishing chaos from random fractal sequences. Nature (London), **358**(6383): 217–220. doi:10.1038/358217a0.

Walters, C. 2003. Folly and fantasy in the analysis of spatial catch rate data. Can. J. Fish. Aquat. Sci. **60**(12): 1433–1436. doi:10.1139/f03-152.

Zainuddin, M., Kiyofuji, H., Saitoh, K., and Saitoh, S.I. 2006. Using multi-sensor satellite remote sensing and catch data to detect ocean hot spots for albacore (*Thunnus alalunga*) in the northwestern North Pacific. Deep Sea Res. Part II Top. Stud. Oceanogr. **53**(3–4): 419–431. doi:10.1016/j.dsr2.2006.01.007.